Soil erosion and sediment delivery in a mountain catchment under scenarios of land use change using a spatially distributed numerical model.

Abstract: Soil erosion and sediment yield are strongly affected by land use/land cover (LULC). Spatially distributed erosion models are of great interest to assess the expected effect of LULC changes on soil erosion and sediment yield. However, they can only be applied if spatially distributed data is available for their calibration. In this study the soil erosion and sediment delivery model WATEM/SEDEM was applied to a small (2.84 km^2) experimental catchment in the Central Spanish Pyrenees. Model calibration was performed based on a dataset of soil redistribution rates derived from point ^{137}Cs inventories, allowing capture differences per land use in the main model parameters. Model calibration showed a good convergence to a global optimum in the parameter space, which was not possible to attain if only external (not spatially distributed) sediment yield data were available. Validation of the model results against seven years of recorded sediment yield at the catchment outlet was satisfactory. Two LULC scenarios where then modeled to reproduce the land use at the beginning of the twentieth Century and a hypothetic future scenario, and to compare the simulation results to the current LULC situation. The results show a reduction of about one order of magnitude in gross erosion (3,180 to 350 Mg yr^{-1}) and sediment delivery (11.2 to 1.2 Mg yr^{-1} ha^{-1}) during the last decades as a result of the abandonment of traditional land uses (mostly agriculture) and subsequent vegetation re-colonization. The simulation also allowed assessing differences in the sediment sources and sinks within the catchment.

Keywords: soil erosion, sediment transport, sediment yield, sediment delivery ratio, sediment sources, land use/land cover changes, Arnás catchment, Spanish Pyrenees.

1. Introduction

According to estimations one sixth of the surface land is affected by accelerated water erosion (Schröter et al., 2005). Apart from the at-site problems related to loss of fertile land, sediment yield to the stream network poses problems for hydraulic infrastructures such as reservoirs, and for the preservation of certain fluvial ecosystems. Mountain regions, where the energy relief contributes to increase soil erosion and sediment redistribution rates, are among the areas at risk. It has been pointed out that land use / land cover (LULC) change is among the main factors explaining the intensity of soil erosion, even exceeding the importance of rainfall intensity and slope in some cases (García-Ruiz, 2010). The effects of LULC change on soil erosion and sediment transport have raised the attention of transnational authorities (e.g., UN, 1994; EC, 2002; COST634, 2005). Many studies have demonstrated that historical LULC change has affected the sediment yield in drainage basins over the World (e.g., Dearing, 1992; Piégay et al., 2004; Cosandey et al., 2005; Gyozo et al., 2005).

The impact of LULC change on soil erosion and sediment yield are well understood qualitatively, but there is still little quantitative knowledge. It has been addressed in different ways: i) field suspended sediment load measurements and historical sedimentary archives (sediment accumulated in lakes) showed that deforestation and changes in the agricultural practices greatly influenced erosion and sediment transport (e.g., Valero-Garcés et al., 2000); ii) experimental catchments have been monitored worldwide in order to understand the factors that control runoff generation and sediment transport (e.g., Bosch and Hewlett, 1982), and to obtain detailed information on different parameters for hydrological modeling and to assess the influence of LULC change on erosion rates and sediment yield (e.g., García-Ruiz et al., 2008). All these studies provided a deep insight into the interaction between LULC change and geomorphic processes. Experimental approaches, however, are resource-intensive and very limited in their ability to address the effects of future changes in LULC or other drivers such as the climate.

Erosion models are useful tools for comparing erosion resulting from current LULC condition with a number of alternative LULC scenarios. Spatially distributed models allow determining not only the variation in the total sediment exported, but also assessing differences in sediment sources and the existence of sedimentation areas at intermediate locations within the watershed. Although most of erosion and sedimentation processes have been studied in detail using experimental devices, assessing the link between on-site soil erosion and total sediment yield at the outlet of a catchment is very difficult because it implies making a complete sediment budget of the catchment including possible internal sedimentation areas, on which there is seldom quantitative data available. Recent advances in spatially distributed erosion and sediment transport models opened new possibilities to understand the complex spatial patterns of erosion and deposition within a catchment (Merrit et al., 2003). However, a direct comparison of predicted erosion rates with field observations, which is necessary for validating the accuracy of the estimates, is usually not possible because it is not practically or financially feasible to acquire long-term, spatially distributed soil erosion data. In the best instances data are available only on the sediment transported by the main rivers in a catchment, and these data seldom span a long time period (Alatorre et al., 2010). For example, it is common to rely on catchment-aggregated soil erosion rates derived from reservoir or lake sedimentation records for the calibration or validation of erosion and sediment transport models (e.g., de Vente et al., 2008). This allows predicting the total catchment sediment yield, but the capability to predict soil redistribution within the catchment is lost. The lack of spatially distributed soil erosion data is a major problem hindering the use of spatially distributed erosion models, and even makes model calibration not possible (Alatorre et al., 2010).

In addition to modeling exercises, the difficulties associated with classical techniques for estimating erosion have led to research into new methods. In the last decades field measurements of fallout cesium-137 (^{137}Cs) inventories have been used to determine soil redistribution rates at specific points in the landscape. Here soil redistribution refers to the net result of erosion and sedimentation over a period of approximately 50 years (Walling and Quine, 1990). The use of fallout radionuclides has attracted increasing attention as an alternative approach for water-induced soil erosion analysis, and it has been applied successfully in a wide range of environments (e.g., Ritchie and McHenry, 1990; Walling and Quine, 1991; Navas & Walling, 1992; Collins et al., 2001; Bujan et al., 2003). Unlike the experimental devices described above, ^{137}Cs soil redistribution estimates are related to a small sampling surface (usually a few dm^2), and can be taken as point estimates when considered at the landscape scale.

A simple approach for studying spatial patterns of soil redistribution from point ^{137}Cs estimates is to get a sufficiently large sample and perform a spatial interpolation. ^{137}Cs-derived soil redistribution rates have also been used for validating the results of process-based erosion models, including: i) empirical erosion models such as the Revised Universal Soil Loss Equation (RUSLE) (Ferro et al., 1998; López-Vicente et al., 2008); ii) spatially semi-distributed erosion models such as the Aerial Non-point Source Watershed Environmental Response Simulation (ANSWERS) and the Agricultural Non-point Source Pollution (AGNPS) (De Roo, 1993; Walling et al., 2003); and iii) fully spatially distributed physically based models such as the Limburg Soil Erosion Model (LISEM) and WATEM/SEDEM (Takken et al., 1999; Feng et al., 2010).

The main objective of the present study was to assess soil redistribution and sediment supply to the stream network under land abandonment on a mountain catchment, using a spatially distributed model (WATEM/SEDEM) combined with ^{137}Cs-derived soil redistribution estimates. The study area (the Arnás catchment in the Spanish Pyrenees) is an experimental area for which a good amount of data and process-knowledge exists, including sediment yield data at the catchment outlet that could be used for validation (Lana-Renault et al., 2007b). In addition, ^{137}Cs-derived soil redistribution rates were available from a previous study (Navas et al., 2005), allowing spatially distributed model calibration under the current LULC situation. Two LULC scenarios were then modeled reproducing the land use at the beginning of the twentieth Century and a hypothetic future scenario, and the results compared to the current situation. We discuss the validity of the results and their application. The approach followed is transferable to other regions of the World.

2. Materials and methods

2.1 Hillslope sediment delivery model

We used WATEM/SEDEM to model soil erosion and sediment flux from the hillslopes to the stream network in a small mountain catchment under current, past and hypothetical land use. WATEM/SEDEM is a spatially-distributed soil erosion and sediment transport model based on the RUSLE model plus a sediment transport capacity equation and a cascading transport model, for predicting sediment delivery to the stream network (Van Oost et al., 2000; Van Rompaey et al., 2001; Verstraeten et al., 2002). WATEM/SEDEM has been used in various types of environments in (Van Rompaey et al., 2001; Verstraeten et al., 2002; Van Rompaey et al., 2003a, 2003b, 2005; Verstraeten et al., 2007), including hydrological catchments in Spain (de Vente et al., 2008; Alatorre et al., 2010).

The models starts by calculating annual soil erosion rates following the RUSEL approach (Renard et al., 1991):

$$E = R\ K\ LS_{2D}\ C\ P\ , \qquad (1)$$

where E is the mean annual soil loss (kg m^{-2} y^{-1}), R a rainfall erosivity factor (MJ mm m^{-2} h^{-1} yr^{-1}), K a soil erodibility factor (kg h MJ^{-1} mm^{-1}), LS_{2D} a slope-length factor (Desmet and Govers, 1996), C a dimensionless crop management factor, and P a dimensionless erosion control practice factor. Next the sediment generated is routed downslope according to the topography until a stream cell is reached. Sediment transport by overland runoff is modeled according to a transport capacity equation (Van Rompaey et al., 2001):

$$TC = ktc\ R\ K \left(LS_{2D} - 4.1 s^{0.8}\right), \qquad (2)$$

where *TC* is the transport capacity (kg m^{-1} yr^{-1}), *s* the slope gradient (m m^{-1}), and *ktc* (m) an empirical transport capacity coefficient that depends on the land cover. A mass balance approach is followed for determining the net amount of sediment in each cell: the sediment transported to the cell from neighboring upslope cells is added to the sediment generated in-cell by erosion, and this amount is then exported entirely to the downslope cells (if it is lower than the transport capacity) or deposited in the cell (if it is greater than the transport capacity). Although several equations exist for the transport capacity in cases where gully erosion dominates (e.g. Verstraeten et al., 2007), we used the original formulation because sheet wash erosion is the main erosion process in our study area.

The parameter *ktc* in equation (2) represents the slope length needed to produce an amount of sediment equal to a bare surface with identical slope gradient, and varies between extreme values of 0 and 1 (Verstraeten, 2006). It depends on the land cover, and it is assumed to vary linearly between arable land highly prone to erosion where *ktc* is highest and densely vegetated areas less prone to erosion where *ktc* is lowest (Van Rompaey et al., 2001, 2005). This implies that *ktc* is site-dependent and needs to be calibrated based on experimental data for each application of the model. Calibration of *ktc* requires determining the optimum value of the two values ktc_{min} and ktc_{max} based on observed erosion data. Since these values depend on the land cover, erosion data for different land cover types is needed for calibrating *ktc*. This data is seldom available, since in the best cases sediment yield data at the catchment outlet is the only data at hand. It has been proposed that a fixed ratio between values ktc_{max} and ktc_{min} can be taken (Verstraeten, 2006), thus reducing the problem to calibrating only one parameter, but there are no easy ways to decide which is the most appropriate value for that ratio, since it is site-dependent.

In this work we used soil redistribution rates derived from fallout cesium-137 (^{137}Cs) as a method for calibrating ktc_{min} and ktc_{max}. The ^{137}Cs technique is based on a comparison of measured inventories (activity per unit area) at individual sampling points with a measured reference inventory at stable sites in the same catchment. Soil redistribution rates are estimated from the difference between those values using a mass balance model and considering both the fallout rates and natural decay of the radioisotope over the time span (Soto and Navas, 2004). A major advantage of the ^{137}Cs technique is the potential to provide medium-term (40 to 50 years, depending on the sampling date), spatially distributed information regarding net soil redistribution (erosion and aggradation) rates. Additionally, and with the objective of illustrating the discussion about the model calibration, we performed an alternative calibration based on seven years of sediment yield recorded at the catchment outlet. Details of the ^{137}Cs and sediment yield datasets and of the calibration procedure are given in the following sections.

2.2 Study area

The Arnás catchment is located in the Borau valley, central Spanish Pyrenees, in the headwaters of the Aragón River (Figure 1A). The catchment is an experimental site area that has been subject of many studies. It has been described in detail in several works, for example in Navas et al. (2005). Here we will outline its main characteristics.

The catchment covers an area of 2.84 km^2, with altitudes between 912–1339 m above the sea level (Figure 1B and 1C). The climate is sub-Mediterranean with Atlantic influence, with average temperature of 10 ºC and average annual precipitation of 930 mm for the period October 1996 to September 2009. Precipitation is slightly higher in autumn and spring due to frontal activity. Nevertheless, snowfall is not rare during the winter, and some storms occur in summer. Snow remains on the soil only for a few days per year, since the 0 ºC isotherm is located above 1600 m a.s.l. during winter.

The area is underlain by Eocene flysch, i.e. by alternating layers of marls and sandstone. The two slopes of the catchment have contrasting physiographic characteristics. On the southwest-facing slopes, poorly developed Rendsic Leptosols and Calcaric Regosols on unconsolidated materials predominate (Navas et al., 2005), with an average slope gradient of 0.5 m m^{-1}. On these steep slopes several ancient mass movements (debris flows) are identified, disconnected from the fluvial network (Lorente et al., 2000), and having a scarce influence on the sediment load at the basin scale (Bathurst et al., 2007). On the gentler northeast-facing slope (average gradient of 0.28 m m^{-1}), soils are haplic Kastanozems and Phaeozems. These soils are deeper (50 to >75 cm) and better developed with clearly differentiated soil horizons (Navas et al., 2005). Some deep mass movement (earthflows) affected the slope, resulting in an undulated topography and in some small wet areas. The low slope gradient (average 0.08 m m^{-1}) on the valley bottom has deep Calcaric Fluvisols developed on alluvial deposits, with minimal horizon differentiation (Navas et al., 2005). The main soil properties are summarized in Table 1.

Vegetation is composed of Mediterranean shrubs (*Buxus sempervirens, Genista scorpius*) on the south-west facing slope (shrub slope), and *Juniperus communis, Buxus sempervirens, Echynospartum horridum* and forest patches with *Pinus sylvestris* in the north-east facing slope (forest slope) (Figure 1E). For centuries, land use in the Arnás catchment consisted on farming both the northeast- and southwest-facing slopes, in very difficult topographic conditions. Commonly, the shady aspect was not cultivated in the Pyrenees, whereas the south facing slopes were cultivated up to 1600 m a.s.l. (García-Ruiz and Lasanta, 1990). Exceptionally, the Arnás catchment was also farmed in the north-east facing slope due to its smooth gradient, allowing a relatively high insolation for cereal cropping in sloping fields. Concave slopes in the sunny slope were occupied with bench terraces, while the convex and straight slopes were cultivated under shifting agriculture systems with scarce practices of soil conservation (Lasanta et al., 2006). Since the beginning of the 20th century, farmland abandonment firstly affected the worst fields under shifting agriculture. Since the 1950's the rest of the sloping and bench terraced fields were also abandoned, and the flat fields in the valley bottom were abandoned in the 1970's. As a consequence of land abandonment a complex process of plant colonization occurred, resulting in the installation of dense shrub communities and an increasing presence of trees. The fields in the valley bottom still remain as grazing meadows, although *Genista scorpius* is progressively colonizing them due to very low grazing pressure. The process described is similar to that observed in other European regions in which re-vegetation processes are the consequence of land abandonment (Kozak, 2003; Taillefumier and Piégay, 2003; Torta, 2004).

Since 1996 a number of studies have been carried out in the Arnás catchment devoted to understanding its hydrology, soil properties and processes (Navas et al., 2002a; Navas et al., 2002b; Seeger et al., 2004; García-Ruiz et al., 2005; Navas et al., 2005; Lana-Renault et al., 2007a; Lana-Renault et al., 2007b; Lana-Renault and Regüés, 2007; Navas et al., 2008; Lana-Renault and Regüés, 2009; López-Vicente et al., 2011).

2.3 Data

An input dataset was prepared as GIS layers with a 5x5 m horizontal resolution. A digital elevation model (DEM) was the main input, from which a drainage network map was derived by setting a threshold upstream catchment area. Land use, rainfall erosivity, soil erodibility, and crop management maps were also produced based on aerial photo interpretation, daily rainfall data, and a soil field survey (Figure 2). Detailed information about the development of this dataset is provided as supplementary material.

For calibrating the *ktc* parameter a dataset of 19 ^{137}Cs inventories was used. They were collected along three representative transects: i) five sample points on the south-west facing slope (forest slope); ii) four sample points on the north-east facing slope (shrub slope); and, iii) ten sample points along the valley bottom (Table 3 and Figure 1). Soil redistribution rates were computed at these points by comparing these samples with a reference ^{137}Cs inventory for the area taken on a flat area not affected by erosion or deposition. These are average values for the period between 1963 (starting of significant ^{137}Cs fallout in the region) and 2003 (time of sample collection and radio-isotopic analysis). We refer the interested reader to the article by Navas et al. (2005), where details of the development and interpretation of the ^{137}Cs dataset are given.

In addition, seven years (from October 1999 to September 2008) of sediment yield recorded at the catchment outlet were used for validating the results of the simulation with an independent dataset. Detailed information about the instrumentation and data collected in the Arnás catchment is given in Lana-Renault and Regüés (2009). We also used the sediment yield data to perform an exercise by comparing the calibration obtained from ^{137}Cs (internal) data with a calibration based on catchment yield (external) data.

3. Results

3.1. Model calibration and validation

The calibration procedure consisted in performing a high number of simulations (n=100) corresponding to the time span 1963-2003 modifying the values of ktc_{max} and ktc_{min} at discrete steps within a predefined range. For each combination of ktc_{max} and ktc_{min} a soil erosion map was obtained in terms of net soil redistribution (Mg ha^{-1} y^{-1}), allowing comparison of the point ^{137}Cs soil redistribution estimates with the model simulations for the 5x5 m grid cell corresponding to the location of the ^{137}Cs measurements. The Nash-Sutcliffe model efficiency statistic NS (Nash and Sutcliffe, 1970) was used as a likelihood metric. The relative root mean square error (*RRMSE*) was used as an estimate of the model accuracy. Formulation of the two statistics is given in the supplementary material section.

It was found that the error surfaces varied quite smoothly, allowing construction of a meta-model of the NS and RRMSE statistics in the (ktc_{max}, ktc_{min}) space using thin plate spline interpolation over the 100 simulation runs. Leave-one-out cross-validation of the meta-model yielded a standard error of 0.000344, that is, around 0.1%, and the R^2 of the regression line between TPS cross-validation residuals and measured NS values was 0. These values allow assuming that uncertainty of the meta-model did not affect the estimation of the optimum parameter combination. Thus, the meta-model was analyzed to determine the optimum values of ktc_{max} and ktc_{min} as those that maximized the NS statistic or minimized the RRMSE.

The error surface topographies in the 2D (ktc_{max}, ktc_{min}) space are shown in Figure 3. In both cases a good convergence of the model to a global optimum point coinciding with the maximum NS and the minimum RRMSE values was found, corresponding to values of ktc_{max} = 9.84 m and ktc_{min} = 2.05 m (ratio = 0.208). The model efficiency statistics for these parameters was NS = 0.845 and RRMSE = 0.485, which can be considered very good. There were no problems in identifying the optimum parameter values, since the error surfaces were smooth and converged to a single optimum value. Under these conditions, it is possible to implement an automated algorithm for finding the optimum parameter set in a small number of steps, up to a desired precision. The results shown in Figure 3 demonstrate that the use of spatially distributed sediment yield data from ^{137}Cs inventories allowed calibrating the empirical parameters of WATEM/SEDEM in a satisfactory way.

Application of the calibrated model to the Arnás catchment allowed comparing the soil redistribution rates predicted by WATEM/SEDEM and the corresponding ^{137}Cs estimates (Figure 4). It must be stressed, however, that the comparison made in Figure 5 does not correspond to an independent test, since the ^{137}Cs redistribution rates were used for calibrating the model. The results revealed a strong relationship between both erosion rates (R^2 = 0.503, 0.818 excluding two outlier points), mainly at the points located on the southwest-facing slope (shrub slope) and at the valley bottom. In general, WATEM/SEDEM overestimated slightly the net erosion rates, but this was due to a few influential points. Two points which corresponded to the northeast-facing slope (forest slope), points 5 and 2, were located far from the perfect adjustment line. While WATEM/SEDEM predicted high erosion or sedimentation rates at these points, they can be considered approximately stable as derived from ^{137}Cs estimates. It was possible to obtain stable results for these points by manually tuning the ktc_{min} parameter to a very low value, but this affected negatively the overall calibration.

An alternative calibration was performed based on seven years of sediment yield data at the Arnás catchment outlet. Contrary to the calibration based on ^{137}Cs data, the results of this calibration were not conclusive, since an infinite number of possible parameter combinations could be found that yield equally good results. This is shown as a ‘valley’ in the RRMSE plot or a ‘ridge’ in the NS plot (Figure 5). Differences between these alternative parameter combinations are related to the relative contributions of different land cover types, which could not be assessed without spatially distributed soil erosion data within the catchment.

Data from seven years of hydrological monitoring were used for validating the model. Sediment yield values predicted by WATEM/SEDEM with the best parameter set were compared with sediment yield values measured at the catchment outlet (Lana-Renault and Regüés, 2009). In this case the two samples were independent, so a real validation could be performed. Correspondence between the two values was in general very good (Table 3 and Figure 6), with an overall R^2 of 0.857 (0.991 excluding the worst prediction). The model was good at estimating annual sediment yields close to average, but tended to underestimate high sediment yields and overestimate low sediment yields.

The bad results obtained for the hydrological year 2001-2002, for which the measured sediment yield was abnormally low at 71 Mg y^{-1}, are attributed to changes in the channel caused by accumulation of debris after the years 1999-2000 and 2000-2001, which registered abnormally high sediment production due to the occurrence of severe storms responsible for high rainfall erosivity values. These morphological changes modified temporarily the behavior of the stream, reducing its capacity to transport sediment, and were not captured by the simulation. Overall, sediment yield during the measuring period 1999-2008 was 244 Mg y^{-1}, compared to 268 Mg y^{-1} predicted by WATEM/SEDEM.

3.2. Hillslope sediment delivery and major sediment sources

Application of WATEM/SEDEM to the land use conditions prevailing during the period 1963-2003 allowed estimation of the total sediment yield and assessment of the relative contributions of each hillside. WATEM/SEDEM predicted a gross SY of 350 Mg y^{-1}, which can be translated to specific sediment yield SSY of 1.23 Mg ha^{-1} y^{-1}. These values are slightly higher than the average values recorded during seven years at the gauging station at the outlet of the Arnás catchment, which were 273 Mg y^{-1} and 0.96 Mg ha^{-1} y^{-1}, respectively (Lana-Renault and Regüés, 2009). This could be explained by differences in rainfall erosivity (R-factor) for both periods (Table 4): while for the gauging period 1999-2008 rainfall erosivity was 926 MJ mm ha^{-1} h^{-1} y^{-1}, for the period 1963-2003 a higher value of 1217 MJ mm ha^{-1} h^{-1} y^{-1} was registered. This difference in rainfall erosivity can explain the higher SY estimated for the long period.

To assess the sediment delivery ratio (SDR = SY/gross erosion rate; expressed as a percentage) we calculated the gross soil erosion rate (6,521 Mg year^{-1}) as the net soil erosion for the area (*i.e.,* total sediment production) before sediment was routed down the hillslopes to the Arnás ravine. The predicted SDR value at the outlet of the watershed was approximately 5%.

The predicted sediment yield map was used to analyze the major sediment sources in the Árnas catchment (Figure 7). The major sediment sources were located in the south-west facing slope (scrub slope), with an average SSY = 1.49 Mg ha^{-1} y^{-1}, particularly in the straight slopes in the lowest and highest parts of the hillslope, whilst the convex and concave areas were affected by moderate erosion processes; sedimentation prevailed in some concave sectors and in the flat areas of the valley bottom. The north-east facing slope (forest slope) had a value of SSY = 0.69 Mg ha^{-1} y^{-1}, with, in general, low erosion rates and some areas in which sedimentation prevail, following the terraced borders of old cultivated fields. Apart from the land cover and physiographic differences, stoniness was clearly different between both sides of the valley, being on the south-west facing slope (mostly above 400 g kg^{-1}).

3.3. Effect of land use change on soil redistribution patterns and on sediment yield

The robustness of the calibration of *ktc*, with samples corresponding to different land uses gave confidence for applying the model to alternative LULC scenarios. The contemporary land use contains almost no croplands (Fig. 2B), which may result in a bad calibration of *Ktc* for this land use. However, the abundance of other land use types with a comparable C-factor (and hence similar expected values of *Ktc*) reduces the uncertainty and allows applying the model to other LULC scenarios. An analysis was made of the effects of LULC change in the Arnás catchment in soil redistribution and sediment yield by applying WATEM/SEDEM using two LULC scenarios (Figure 8):

i) the first scenario corresponded to the conditions that prevailed on the catchment during the early twentieth century, when the study area was occupied by annual crops, mainly cereals; and

ii) a second scenario consisting on a hypothetical LULC condition in the future, provided that land use will be almost unmanaged and that vegetation colonization will progress on the south-west facing slope (now mostly covered by dense scrub land) that would be occupied by forests.

SY and SSY maps predicted by WATEM/SEDEM for these two alternative LULC scenarios allowed analyzing the effects of past and foreseen LULC changes on soil erosion patterns and total sediment yield in the Arnás catchment (Table 5 and Figure 9). For the past scenario (LULC prior to 1950) the catchment was almost entirely occupied by cereal crop fields. In fact, inspection of a vertical aerial photograph from 1956 confirms that the Arnás catchment was fully cultivated, both in the north-east and the south-west facing slopes, even on steep slope gradients, occasionally under shifting agriculture systems. The SY and SSY values (3,180 Mg y^{-1} and 11.19 Mg ha^{-1} y^{-1}, respectively) obtained using that scenario were extremely high in comparison with the values obtained with the current LULC, representing an increase of approximately 810%. Consequently the SDR was higher than with the current LULC, rising up to 84% (Table 5).

Net erosion areas had predominance over the sedimentation areas under past LULC, and erosion was intense even in the relatively gentle slopes of the northeast-facing slopes (Figure 9A). A higher number of intermediate sedimentation areas also appeared especially in the northeast-facing slope. These bands are related to the presence of plot margins or slightly terraced slopes (now almost completely hidden by vegetation, but still recognizable in the field), which helped reducing the loss of soil towards the river network.

In the second scenario (future situation) an increment of forest and dense scrubland was proposed in the northeast- and southwest-facing slopes, respectively, as a consequence of land use abandonment (Table 4). The SY and SSY predicted values (255 Mg y^{-1} and 0.89 Mg ha^{-1} y^{-1}, respectively) were approximately 38% lower with respect to the current LULC condition, and 1,150% lower than the past LULC scenario. The SDR was very similar to the value obtained with the current LULC (5.15 %). Nevertheless, the gross erosion rate was 32% lower than the current situation. The sediment yield map (Figure 9B) shows a predominance of low erosion values (less that 10 Mg ha^{-1} y^{-1}), and a reduction of the erosion areas. Figure 9B shows a remarkable trend towards: i) a reduction in the sediment sources, even in the south-west facing slope; and ii) a trend to homogenization.

4. Discussion and conclusions

A spatially distributed soil erosion and sediment transport model, WATEM/SEDEM, was applied to simulate soil redistribution in a mountain catchment under current, past and hypothetical future land use/land cover (LULC) conditions. A dataset of soil redistribution rates derived from ^{137}Cs profiles at 19 sampling points within the catchment were used to calibrate the model.

Calibration using ^{137}Cs data was very successful, since it was possible to determine a single combination of the *ktc* parameters (ktc_{max} = 9.84 m, ktc_{min} = 2.05 m) that provided a good fit to the observed soil redistribution rates within the catchment. Only for two locations in the forested slope a disagreement was found between soil redistribution rates obtained by the two methods, probably as a consequence of the relevance in that area of soil creeping processes that are not considered by the model. These results contrast with a similar study by Feng *et al.* (2010), in which they found a poor convergence to a global optimum parameter set and erosion rates estimated by both methods (WATEM/SEDEM and ^{137}Cs) differed considerably. The optimum values for ktc_{min} and ktc_{max} in that case were 6 and 7 respectively, indicating a poor discrimination between LULC types. The poor performance in this study case could be possibly attributed to deficiencies in the sampling design, since farming LULCs were under-represented in the calibration dataset with only 4 sites against 56 sites in well vegetated LULCs, being an important source of bias against farming LULCs in the calibration process. Additionally, the calibration algorithm described was far from optimal, since the multi-dimensionality of the problem was eliminated by keeping the value of some parameters fixed while calibrating other parameters, ignoring likely co-variances among parameters.

An additional calibration exercise was performed based on sediment yield data at the catchment outlet for comparison purposes, since most applications of WATEM/SEDEM up to date have been based on catchment sediment yield data. This raises a fundamental problem, since it is difficult to calibrate land-cover related parameters with sediment yield alone. As a solution, some authors proposed that a fixed ratio between ktc_{max} and ktc_{min} be taken, which has the effect of lumping both parameters into a single one, thus allowing calibration (Verstraeten, 2006). However this raises new concerns, since there is no way to decide which is the most appropriate value for that ratio, which would be site-dependent. In a previous study in the Ésera watershed in the Central Spanish Pyrenees (Alatorre et al., 2010) we found significant problems for calibrating WATEM/SEDEM based on sediment yield data at the catchment level. The results of the calibration experiment in this work confirm that it is not possible to identify a single combination of *ktc* parameters that allows optimize the objective function, hence demonstrating the need for spatially- and land use-distributed soil redistribution data such as that provided by ^{137}Cs data.

Application of WATEM/SEDEM with the optimum parameter set to the Arnás catchment allowed estimating the sediment balance of the catchment. Very good agreement was found between modeled and measured annual sediment yield values at the catchment outlet. The simulation allowed also determining the major sediment sources within the catchment, and the existence of intermediate sediment traps between the hillslopes and the channel network. Mean sediment yield was determined at 350 Mg y^{-1} or 1.23 Mg ha^{-1} y^{-1}. These values are similar in order of magnitude to other catchments in the Spanish Pyrenees. Almorox et al. (1994) obtained an estimate of 4.12 Mg ha^{-1} $year^{-1}$ for the Yesa Reservoir in the Aragón River basin, 1.67 Mg ha^{-1} $year^{-1}$ for Barasona reservoir in the Ésera river basin. Similar or higher values have been estimated for small experimental catchments in the French Alps (Mathys et al., 2005), the Eastern Pyrenees

(Gallart et al., 2005; Soler et al., 2008), and the Central Pyrenees (*García-Ruiz et al.*, 2008), which encompass a variety of bedrocks and climates.

Sediment delivery ratio (SDR) for the catchment was determined at approximately 5%. This is a low value, but not extreme considering the high variability of this parameter among catchments. For example, Van Rompaey et al. (2007) reported a SDR of 28% for a catchment of 1,960 km^2 in the Czech Republic; Verstraeten et al. (2007) found SDR values of 20–39% for catchments of 164–2,173 km^2 in Australia; Fryirs and Brierley (2001) estimated an extremely high SDR of almost 70% in the Bega River catchment (New South Wales, Australia), which caused dramatic changes to the river morphology; Romero Díaz et al. (1992) found SDR values of 7–46% in the subcatchments of the Segura River (Spain); and de Vente et al. (2008) predicted SDR values ranging from 0.03% to 55% for 61 catchments in Spain. It must be noted, however, that the catchments cited are of very varying size and that SDR calculation methods vary between studies, so any comparison must be taken with great care.

The existence of a robust calibration of the model's parameters allowed performing additional simulations under LULC scenarios. Simulation under past land use (farming land in most of the catchment) resulted in an increase of gross erosion and sediment yield of about one order of magnitude. These values coincide with the intensity of erosive processes (mostly sheet wash and rill formation, but also shallow landsliding) that has been described as predominant during the period of maximum agricultural activity (García-Ruiz et al., 1995; García-Ruiz and Valero-Garcés, 1998), resulting in a degraded landscape, surface stoniness and braiding of the stream network (Beguería et al., 2006). The SDR increased up to 84%, and a much better connectivity between erosion areas and the stream network was found. A second LULC cover scenario reproducing an increase of the vegetation cover due to land use abandonment resulted in erosion and sediment yield values approximately one third lower than under current LULC. The SDR was quite similar to the current one.

In the absence of long-term sediment yield records, simulations with WATEM/SEDEM allow quantifying the effect of recent LULC change on the reduction of soil erosion and sediment source areas as a consequence of the abandonment of agricultural activities and vegetation re-colonization. As our simulations suggest, this process has almost reached its final stage, since further increase or densification of the vegetation cover did not have a large effect on either gross erosion or sediment yield values. Although these findings can be translated to other mountain areas, it must be noted that in certain cases land abandonment can increase spatial connectivity and so produce higher sediment yields (García-Ruiz and Lana-Renault, 2011).

As pointed out in previous works (Alatorre et al., 2010), 'spatially lumped models provide reasonable predictions of sediment yield but offer no insight into sediment sources'. A clear advantage of spatially-distributed models is that they can be useful for implementing measures to prevent soil erosion and sediment generation, since they allow assessing the impacts of changes in land use or climate. However, the use of models of this kind usually involves calibration of empirical parameters, so records of soil redistribution rates are required. We have demonstrated that the use of catchment sediment yield data alone is not enough to allow for a robust calibration of land use-dependent parameters. The use of ^{137}Cs-derived soil redistribution rates can provide this information and arises as a very promising technique for the calibration of soil erosion and redistribution models.

In this work we have shown that a spatially-distributed soil erosion and redistribution model can be used for evaluating sediment budgets with current and alternative land use scenarios. We assessed variations in the amount of sediment exported, but also changes in the sediment source and deposition areas as a consequence of past and likely future land use change. Such an assessment has only been possible with the help of internal measurements of soil redistribution such as those provided by a ^{137}Cs survey. We demonstrate that external data such as measurements of total sediment yield at the catchment outlet do not provide enough information for performing a calibration of a distributed model with spatially dependent parameters. This is an important conclusion that should be considered in further applications of such models.

Acknowledgments

This work has been supported by the following research projects: MEDEROCAR (CGL2008-00831/BTE), EROMED (CGL2011-25486) and DISDROSPEC (CGL2011–24185) financed by the Spanish Commission of Science and Technology (CICYT) and FEDER, ChangingRISKS (OPE00446/PIM2010ECR-00726) financed by EU ERA-NET CIRCLE Programme, and Grupo de Excelencia E68 financed by the Aragón Government and FEDER. Research of M. A.-M. Contribution of L.-C. A. was made possible through a scholarship granted by The National Council for Science and Technology of Mexico (CONACYT).

References

Alatorre, L.C., Beguería, S., and García-Ruiz, J.M.: Regional scale modeling of hillslope sediment delivery: a case study in Barasona reservoir watershed (Spain) using WATEM/SEDEM, Journal of Hydrology, 391(1-2), 109-123, 2010.

Almorox, J., De Antonio, R., Saa, A., Cruz, Díaz M., and Gasco, J.M.: Métodos de estimación de la erosión hídrica, Ed. Agrícola Española, Madrid, España, 152 pp., 1994.

Angulo-Martínez M., and Beguería S.: Estimating rainfall erosivity from daily precipitation records: a comparison between methods in the Ebro Basin (NE Spain), Journal of Hydrology, 379, 111–121, 2009

Bathurst, J.C., Moretti, G., El-Hames, A., Beguería S., and García-Ruiz, J.M.: Modelling the impact of forest loss on shallow landslide sediment yield, Ijuez river catchment, Spanish Pyrenees, Hydrology and Earth System Sciences, 11 (1), 569–583, 2007.

Beguería, S., López-Moreno, J.I., Gómez-Villar, A., Rubio, V., Lana-Renault, N., and García-Ruiz, J.M.: Fluvial adjustments to soil erosion and plant cover changes in the Central Spanish Pyrenees, Geografiska Annaler, 88A (3), 177–186, 2006.

Bosch, J.M., and Hewlett, J.D.: A review of catchment experiments to determine the effect of vegetation changes on water yield and evapotranspiration, Journal of Hydrology, 55(1-4), 3–23, 1982.

Bujan, A., Santanatoglia, O.J., Chagas, C., Massobrio, M., Castiglioni, M., Yanez, M., Ciallella, H., and Fernández, J.: Soil erosion evaluation in a small basin through the use of Cs-137 technique, Soil & Tillage Research, 69, 127–137, 2003.

Collins, A.L., Walling, D.E., Sichingabula, H.M., and Leeks, G.J.L.: Using 137Cs measurements to quantify soil erosion and redistribution rates for areas under different land use in the Upper Kaleya River basin, southern Zambia, Geoderma, 104, 229–323, 2001.

Cosandey, C., Andréassian, V., Martin, C., Didon-Lescot, J.F., Lavabre, J., Folton, N., Mathys, N., and Richard, D.: The hydrological impact of the Mediterranean forest: a review of French research, Journal of Hydrology, 301(1-4), 235–249, 2005.

COST634: On- and Off-Site Environmental Impacts of Runoff and Erosion. European Cooperation in the Field of Scientific and Technical Research, Reading, available at: http://www.soilerosion.net/cost634/, 2005.

De Roo, A.P.J.: Validation of the ANSWERS catchment model for runoff and soil erosion simulation in catchment in The Netherlands and the United Kingdom, IAHS Pub., 211, 465–474, 1993.

de Vente, J., Poesen, J., Verstraeten, G., Van Rompaey, A., and Govers, G.: Spatially distributed modelling of soil erosion and sediment yield at regional scales in Spain, Global and Planetary Change, 60, 393–415 2008.

Dearing, J.A.: Sediment yields and sources in a Welsh upland lake-catchment during the past 800 years, Earth Surface Processes and Landforms, 17, 1–22 1992.

Desmet, P.J.J., and Govers, G.: A GIS procedure for automatically calculating the USLE LS factor on topographically complex landscape units, Journal of Soil and Water Conservation, 51, 427–433 1996.

EC: Towards a Thematic Strategy for Soil Protection, Commission of the European Communities, Brussels 2002.

FAO: Soil Map of the World, Revised Legend, FAO, Rome. 1989.

Feng, X., Wang, Y., Chen, L., Fu, B., and Bai, G.: Modeling soil erosion and its response to land-use change in hilly catchments Chinese Loess Plateau, Geomorphology doi:10.1016/j.geomorph.2010.01.004 2010.

Ferro, V., Porto, P., and Tusa, G.: Testing a distributed approach for modeling sediment delivery, Hydrological Sciences Journal, 43 (3), 425–442 1998.

Fryirs, K., and Brierley, G.J.: Variability in sediment delivery and storage along river courses in Bega catchment, NSW, Australia: implications for geomorphic river recovery, Geomorphology, 38, 237–265 2001.

Gallart, F., Balasch, J.C., Regüés, D., Soler, M., and Castelltort, F.: Catchment dynamics in a Mediterranean mountain environment: the Vallcebre research basins (southeastern Pyrenees) II: temporal and spatial dynamics of erosion and stream sediment transport, in: C. García, C., Batalla, R.J., (Eds.), Catchment dynamics and river processes: Mediterranean and other climate regions, Developments in Earth Surface Processes, 7, 17–29, 2005.

García-Ruiz, J.M.: The effects of the land use on soil erosion in Spain: A review, Catena, 81, 1–11, 2010.

García-Ruiz, J.M., and Lasanta-Martínez, T.: Land-use changes in the Spanish Pyrenees, Mountain Research & Development, 10 (3), 267–279, 1990.

García-Ruiz, J.M., Lasanta, T., Ortigosa, L., Ruiz-Flaño, P., Martí, C., and González, C.: Sediment yield under different land uses in the Spanish Pyrenees, Mountain Research & Development, 15 (3), 229–240, 1995.

García-Ruiz, J.M., and Valero-Garcés B.: Historical geomorphic processes and human activities in the Central Spanish Pyrenees, Mountain Research and Development, 18 (4), 309–320, 1998.

García-Ruiz, J.M., Arnáez, J., Beguería, S., Seeger, M., Martí-Bono, C., Regüés, D., Lana-Renault, N., and White, S.: Runoff generation in an intensively disturbed, abandoned farmland catchment, Central Spanish Pyrenees, Catena, 59 (1), 79–92, 2005.

García-Ruiz, J.M., Regües, D., Alvera, B., Lana-Renault, N., Serrano-Muela, P., Nadal-Romero, E., Navas, A., Latron, J., Martí-Bono, C., and Arnáez, J.: Flood generation and sediment transport in experimental catchments along a plant cover gradient in the Central Pyrenees, Journal of Hydrology, 356, 245–260, 2008.

García-Ruiz, J.M., and Lana-Renault, N.: Hydrological and erosive consequences of farmland abandonment in Europe, with special reference to the Mediterranean region - A review, Agriculture, Ecosystems and Environment, 140, 317-338, 2011.

Gyozo, J., van Rompaey, A., Szilassi, P., Csillang, G., Mannaerts, C., and Woldai, T.: Historical land use changes and their impact on sediment fluxes in the Balaton basin (Hungary), Agriculture, Ecosystems and Environment, 108, 119–133, 2005.

Kozak, J.: Forest cover change in the Western Carpathians in the past 180 years: A case study in the Orawa region in Poland, Mountain Research and Development 23 (4), 369–375, 2003.

Lana-Renault, N., Latron, J., and Regüés, D.: Streamflow response and water-table dynamics in a sub-Mediterranean research catchment (Central Spanish Pyrenees), Journal of Hydrology, 347 (3-4), 497–507, 2007a.

Lana-Renault, N., Regüés, D., Martí-Bono, C., Beguería, S., Latron, J., Nadal, E., Serrano, P., and García-Ruiz, J.M.: Temporal variability in the relationships between precipitation, discharge and suspended sediment concentration in a small Mediterranean mountain catchment, Nordic Hydrology, 38 (2), 139–150, 2007b.

Lana-Renault, N., and Regüés, D.: Bedload transport under different flow condition in a human-disturbed catchment in the Central Spanish Pyrenees, Catena, 7 (1), 155–163, 2007.

Lana-Renault, N., and Regüés, D.: Seasonal patterns of suspended sediment transport in an abandoned farmland catchment in the central Spanish Pyrenees, Earth Surface Processes and Landforms 34 (9), 1291–1301, 2009.

Lasanta, T., Beguería, S., and García-Ruiz, J.M.: Geomorphic and hydrological effects of traditional shifting agriculture in a Mediterranean mountain, Central Spanish Pyrenees, Mountain Research and Development, 26 (2), 146–152, 2006.

López-Vicente, M.L., Navas, A., and Machín, J.: Identifying erosive periods by using RUSLE factors in mountain fields of the Central Spanish Pyrenees, Hydrology and Earth System Sciences, 12, 523–535, 2008.

López-Vicente, M., Lana-Renault, N., García-Ruiz, J.M., Navas, A.: Assessing the potential effect of different land cover management practices on sediment yield from an abandoned farmland catchment in the Spanish Pyrenees, Journal of Soils and Sediments 11: 1440–1455, 2011.

Lorente, A., Martí-Bono, C., Beguería, S., Arnáez, J., and García-Ruiz, J.M.: La exportación de sedimento en suspensión en una cuenca de campos abandonados, Pirineo central español, Cuaternario y Geomorfología, 14 (1-2), 21–34, 2000.

Mathys, N., Klotz, S., Esteves, M., Descroix, L., and Lapetite, J.M., Runoff and erosion in the Black Marls of the French Alps: Observations and measurements at the plot scale, Catena, 63, 261–281, 2005.

Merritt, W.S., Letcher, R.A., Jakeman, A.J.: A review of erosion and sediment transport models, Environmental Modelling and Software, 18, 761–799, 2003.

Nash, J.E., and Sutcliffe, J.V.: River flow forecasting through conceptual models: Part 1: a discussion of principles, Journal of Hydrology, 10, 282–290, 1970.

Navas, A., Walling, D.: Using caesium-137 to assess sediment movement in a semiarid upland environment in Spain, in: Walling, D.E., Davies, T.R., Hasholt, B., (Eds.), Erosion, Debris Flows and Environment in Mountain Regions, International Association Hydrological Sciences (IAHS), Publ. nº 209, 129-138, 1992.

Navas, A., Soto, J., and Machín, J.: Edaphic and physiographic factors affecting the distribution of natural gamma-emitting radionuclides in the soil of the Arnás catchment in the Central Spanish Pyrenees, European Journal of Soil Science, 53, 629–638, 2002a.

Navas, A., Soto, J., Machín, J.: 238U, 226Ra, 210Pb, 232Th and 40K activities in soil profiles of the Flysch sector (Central Spanish Pyrenees), Applied Radiation and Isotopes, 57 (4), 579–589, 2002b.

Navas, A., Machín, J., and Soto, J.: Assessing soil erosion in a Pyrenean mountain catchment using GIS and fallout ^{137}Cs. Agriculture, Ecosystems and Environment, 105 (3), 493–506, 2005.

Navas, A., Machín, J., Beguería, S., López-Vicente, M., and Gaspar, L., Soil properties and physiographic factors controlling the natural vegetation re-growth in a disturbed catchment of the Central Spanish Pyrenees, Agroforestry Systems, 72, 173–185, 2008.

Piégay, H., Walling, D.E., Landon, N., He, Q., Liebault, F., and Petiot, R.: Valley landscape, morphology and sedimentation as indicators of recent changes in sediment yield in an Alpine montane basin (The Upper Drôme in France), Catena, 55, 183-212, 2004.

Renard, K.G., Foster, G.R., Weesies, G.A, and Porter, J.P.: RUSLE-revised universal soil loss equation, Journal of Soil and Water Conservation, 46, 30–33, 1991.

Ritchie, J.C., McHenry, J.R.: Application of radioactive fallout cesium-137 for measuring soil erosion and sediment accumulation rates and patterns: a review, Journal of Environmental Quality, 19, 215–233, 1990.

Romero Díaz, M.A., Cabezas, F., and López Bermúdez, F.: Erosion and fluvial sedimentation in the River Segura Basin (Spain), Catena, 19, 379–392, 1992.

Römkens, M., Prasad, J., and Poesen, J.: Soil erodibility and properties, Transactions of the XIII Congress of International Society of Soil Science, vol. V, p. 492– 504, 1987.
Ruiz-Flaño, P., García-Ruiz, J.M., and Ortigosa, L.: Geomorphological evolution of abandoned fields: A case study in the Central Pyrenees, Catena, 19, 301–308, 1992.
Schröter, D., Cramer, W., Leemans, R., Prentice, I.C., Araujo, M.B., Arnell, N.W., Bondeau, A., Bugmann, H., Carter, T.R., Gracia, C.A., de la Vega-Leinert, A.C., Erhard, M., Ewert, F., Glendining, M., House, J.I., Kankaanpaa, S., Klein, R.J.T., Lavorel, S., Lindner, M., Metzger, M.J., Meyer, J., Mitchell, T.D., Reginster, I., Rounsevell, M., Sabate, S., Sitch, S., Smith, B., Smith, J., Smith, P., Sykes, M.T., Thonicke, K., Thuiller, W., Tuck, G., Zaehle, S., and Zierl, B.: Ecosystem service supply and vulnerability to global change in Europe, Science, 310 (5752), 1333–1337, 2005.
Seeger, M., Errea, M.P., Beguería, S., Arnáez, J., Martí, C., and García-Ruiz, J.M.: Catchment soil moisture and rainfall characteristics as determinant factors for discharge/suspended sediment hysteretic loops in a small headwater catchment in the Spanish Pyrenees, Journal of Hydrology 288, 299–311, 2004.
Soler, M., Latron, J., and Gallart, F.: Relationships between suspended sediment concentrations and discharge in two small research basins in a mountainous Mediterranean area (Vallcebre, Eastern Pyrenees), Geomorphology, 98, 143–152, 2008.
Soto, J., and Navas, A.: A model of ^{137}Cs activity profile for soil erosion studies in uncultivated soils of Mediterranean environments, Journal of Arid Ecosystems, 59, 719–730, 2004.
Taillefumier, F., and Piégay, H.: Contemporary land use changes in prealpine Mediterranean mountains: A multivariate gis-based approach applied to two municipalities in the Southern French Prealps, Catena, 51 (3-4), 267–296, 2003.

Takken, I., Beuselinck, L., Nachtergaele, J., Govers, G., Poesen, J., and Degraer, G.: Spatial evaluation of physically-based distributed erosion model LISEM, Catena, 37, 431–447, 1999.

Torta, G.: Consequences of rural abandonment in a Northern Apennines Landscape (Tuscany, Italy), in:S. Mazzoleni et al., (Eds.), Recent dynamics of the Mediterranean vegetation and landscape, Wiley, Chichester, pp. 157–167, 2004.

UN: United Nations Convention to Combat Desertification in those Countries Experiencing Serious Drought and/or Desertification, Particularly in Africa, Paris, 1994.

Valero-Garcés, B., Navas, A., Machín, J., Stevenson, T., and Davis, B.: Responses of a saline lake ecosystem in semi-arid regions to irrigation and climate variability, The history of Salada Chiprana, Central Ebro Basin, Spain, Ambio, 26 (6), 344–350, 2000.

Van Oost, K., Govers, G., and Desmet, P.J.J.: Evaluating the effects of landscape structure on soil erosion by water and tillage, Landscape Ecology, 15(6), 579–591, 2000.

Van Rompaey, A.J.J., Verstraeten, G., Van Oost, K., Govers, G., and Poesen, J.: Modelling mean annual sediment yield using a distributed approach, Earth Surface Processes and Landforms, 26, 1221– 1236, 2001.

Van Rompaey, A., Krasa, J., Dostal, T., and Govers, G.: Modelling sediment supply to rivers and reservoirs in Eastern Europe during and after the collectivization period, Hydrobiologia 494, 169–176, 2003a.

Van Rompaey, A., Verstraeten, G., Van Oost, K., Rozanov, A., Govers, G., and Poesen, J.: Modelling sediment fluxes in the Jonkershoek catchment. Part 1: model calibration and validation, Proceedings of the workshop Cartographic modeling of and degradation, Ghent, Belgium, pp. 75–89, 2003b.

Van Rompaey, A., Bazzoffi, P., Jones, R.J.A., and Montanarella, L.: Modelling sediment yields in Italian catchments, Geomorphology, 65, 157–169, 2005.

Van Rompaey, A., Krasa, J., and Dostal, T.: Modelling the impact of land cover changes in the Czech Republic on sediment delivery, Land Use Policy, 24, 576–583, 2007.

Verstraeten, G., Van Oost, K., Van Rompaey, A., Poesen, J., and Govers, G.: Evaluating an integrated approach to catchment management to reduce soil loss and sediment pollution through modeling, Soil Use and Management 18, 386–394, 2002.

Verstraeten, G.: Regional scale modelling of hillslope sediment delivery with SRTM elevation data, Geomorphology, 81, 128–140, 2006.

Verstraeten, G., Poesen, J., Gillijns, K., and Govers, G.: The use of riparian vegetated filter strips to reduce river sediment loads: an over-estimated control measure?, Hydrological Processes, 20, 4259–4267, 2006.

Verstraeten, G., Prosser, I.P., and Fogarty, P.: Predicting the spatial patterns of hillslope sediment delivery to river channels in the Murrumbidgee catchment, Australia, Journal of Hydrology, 334 (3–4), 440–454, 2007.

Walling, D.E., and Quine, T.A.: Calibration of Cs-137 measurements to provide quantitative erosion rate data, Land Degradation and Rehabilitation, 2, 161–175, 1990.

Walling, D.E., and Quine, T.A.: Use of 137-Cs measurements to investigate soil erosion on arable fields in the UK: potential applications and limitations, European Journal of Soil Science, 42, 147–165, 1991.

Walling, D.E., He, Q., and Whelan, P.A.: Using ^{137}Cs measurements to validate the application of the AGNPS and ANSWERS erosion and sediment yield models in two small Devon catchments, Soil & Tillage Research, 69, 27–43. 2003.

Table 1. Principal soil characteristics of the two valley sides in the Arnás catchment (mean ±standard deviation over the whole soil profile), adapted from Navas et al. (2005).

	Northeast-facing slope (forest), n=48	Southwest-facing slope (shrub), n=29
pH	7.97 (±0.42)	8.17(±0.19)
Clay (g kg^{-1})	210 (±31)	195 (±34)
Silt (g kg^{-1})	660 (±63)	620 (±73)
Sand (g kg^{-1})	130 (±85)	180 (±103)
Organic matter (g kg^{-1})	59 (±22)	54 (±25)
Bulk density (g kg^{-1})	1.12 (±1.22)	1.19 (±0.61)
Moisture (%)	17 (±6.7)	11 (±7.7)
Porosity (%)	57 (±5.9)	55 (±6.2)

Table 2. 137Cs inventories and derived soil redistribution rates for the period 1963-2003 along three transects in the Arnás catchment (Navas et al., 2005): negative and positive values indicate net soil erosion and aggradation, respectively. Location of the ^{137}Cs inventories is shown in Fig. 1D.

Transect	Point ID	^{137}Cs inventory (m Bq cm^{-2})	Soil redistribution (Mg ha^{-1} year^{-1})
Forest	1	437	0.9
Forest	2	400	0
Forest	3	430	0.8
Forest	4	404	0.1
Forest	5	400	0
Shrub	6	175	-26.4
Shrub	7	162	-29.5
Shrub	8	280	-11.6
Shrub	9	282	-14.3
Valley	10	297	-7.4
Valley	11	367	-2.0
Valley	12	476	2.2
Valley	13	433	1.0
Valley	14	436	1.0
Valley	15	324	-4.3
Valley	16	439	1.2
Valley	17	325	-5.2
Valley	18	333	-4.7
Valley	19	248	-44.6

Table 3. Values of cumulative precipitation (P), runoff coefficient (RC), rainfall erosivity (R factor), measured sediment yield (Obs. SY) and specific sediment yield (Obs. SSY) in the Arnás experimental catchment (adapted from Lana-Renault and Regüés, 2009), rainfall erosivity (R-factor) calculated from high frequency (15 minutes) rain gauge data (Angulo-Martínez and Beguería, 2009) and simulated sediment yield (Sim. SY and Sim. SSY). Annual values for the hydrological years between 1999-2000 and 2007-2008, and averages for the periods 1999-2008 and 1963-2003. NA (not available) indicates that no data exists for a given parameter and time period.

Year (Oct-Sep)	P (mm)	RC (mm mm^{-2})	R-factor (MJ mm ha^{-1} h^{-1} y^{-1})	Obs. SY (Mg y^{-1})	Obs. SSY (Mg ha^{-1} y^{-1})	Sim. SY (Mg y^{-1})	Sim. SSY (Mg ha^{-1} y^{-1})
1999-2000	881	0.42	1302	542	1.91	473	1.67
2000-2001	1353	0.35	1216	381	1.34	348	1.22
2001-2002	765	0.14	852	71	0.25	244	0.86
2002-2003	1043	0.20	792	216	0.76	227	0.80
2003-2004	958	0.33	846	253	0.89	242	0.85
2005-2006	986	0.25	715	116	0.41	155	0.55
2007-2008	922	0.30	754	129	0.45	186	0.65
1999-2008	986	0.28	926	244	0.86	268	0.94
1963-2003	925	NA	1217	NA	NA	350	1.23

Table 4. Predicted gross erosion, sediment yield (SY), specific sediment yield (SSY) and sediment delivery ratio (SDR) under current land cover / land use (LULC) conditions and two LULC scenarios (prior to 1950 and future) in the Arnás catchment, based on the best parameterization of ktc_{max} and ktc_{min} over the period 1963-2003.

Period	Gross erosion ($Mg\ y^{-1}$)	SY ($Mg\ y^{-1}$)	SSY ($Mg\ ha^{-1} y^{-1}$)	SDR (%)
Current LULC	6,521	350	1.23	5.36
LULC before 1950	32,066	3,180	11.19	9.90
LULC future scenario	4,947	255	0.89	5.15

Figure captions

Figure 1. Study area: A) location of the Arnás catchment; B) map of the Arnás catchment showing the sites of the main monitoring instruments and soil samples; C) Lithologic map and location of the ^{137}Cs profiles (see points IDs in Table 3); D) digital terrain model (DTM) and ^{137}Cs inventories (m Bq cm^{-2}); and E) current land cover/land use map derived from aerial photo-interpretation.

Figure 2. Input data derived from the database of the Arnás catchment: A) drainage network map derived from the DTM using threshold value of 1 km^2 contributing area (continuous line); B) parcel map, derived from the current land use/land cover map; C) soil erodibility map (K-factor in RUSLE, Mg h MJ^{-1} mm^{-1}); and D) crop management map (C-factor in RUSLE).

Figure 3. Calibration of the transport capacity parameters ktc_{min} and ktc_{max} (m) using ^{137}Cs soil redistribution rates: error surface topographies as measured by the *NS* (left) and the *RRMSE* (right) statistics on the two-dimensional space determined by both parameters. Green colour represents the best fit.

Figure 4. Results of the calibration process: comparison of WATEM/SEDEM and ^{137}Cs soil redistribution estimates for the best parameter set. The solid lines represents a perfect fit, and the dashed one is the linear regression between both datasets.

Figure 5. Calibration of the transport capacity parameters ktc_{min} and ktc_{max} (m) using seven years of sediment yield data at the Arnás catchment outlet: error surface topographies as measured by the *NS* (left) and the *RRMSE* (right) statistics on the two-dimensional space determined by both parameters. Green colour represents the best fit.

Figure 6. Comparison of measured and predicted sediment yield at the Arnás catchment outlet between the hydrological years 1999-2000 and 2007-2008 (October to September). The line 1:1 represents a perfect fit, and the dashed line is the linear regression between both values.

Figure 7. Predicted sediment delivery map of the Arnás catchment under current land use / land cover.

Figure 8. Past (left) and future (right) land use scenarios used in the simulation.

Figure 9. Predicted sediment delivery maps of the Arnás catchment: A) under land use / land cover system at the beginning of the 20th century; and, B) under a likely future LULC system.

824 **Figure 1**

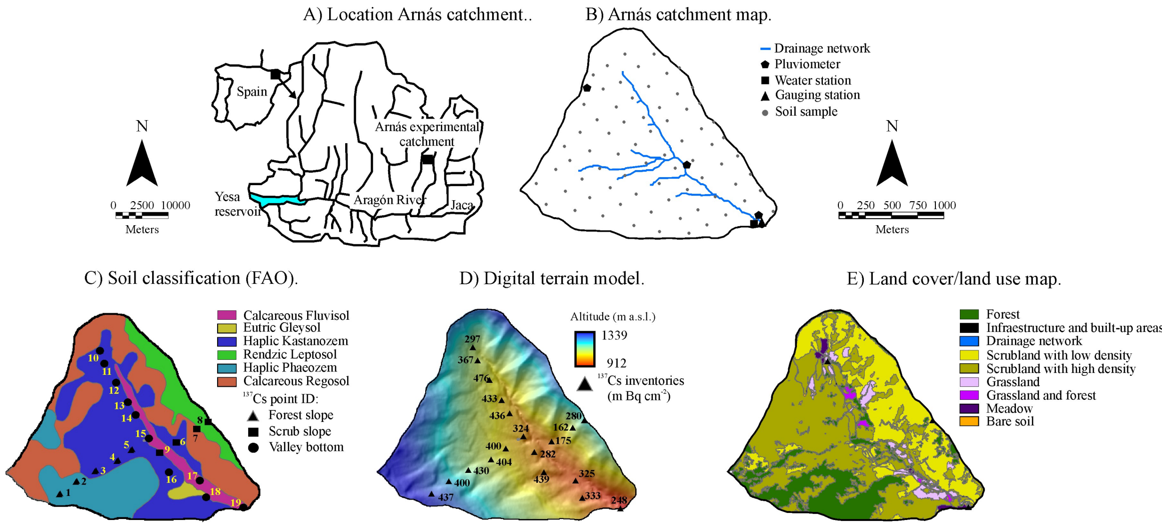

825

826

Figure 2

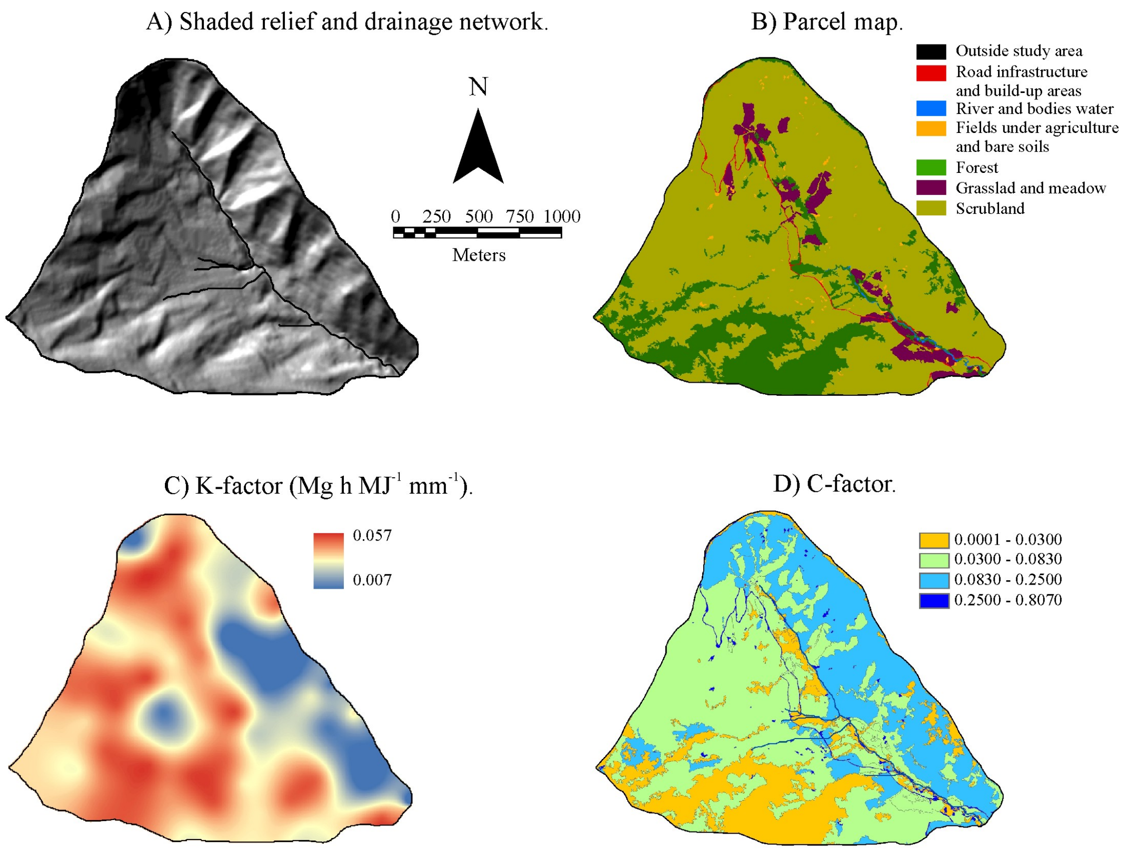

A) Shaded relief and drainage network.
N
0 250 500 750 1000
Meters
B) Parcel map.
Outside study area
Road infrastructure and build-up areas
River and bodies water
Fields under agriculture and bare soils
Forest
Grasslad and meadow
Scrubland
C) K-factor (Mg h MJ^{-1} mm^{-1}).
0.057
0.007
D) C-factor.
0.0001 - 0.0300
0.0300 - 0.0830
0.0830 - 0.2500
0.2500 - 0.8070

Figure 3

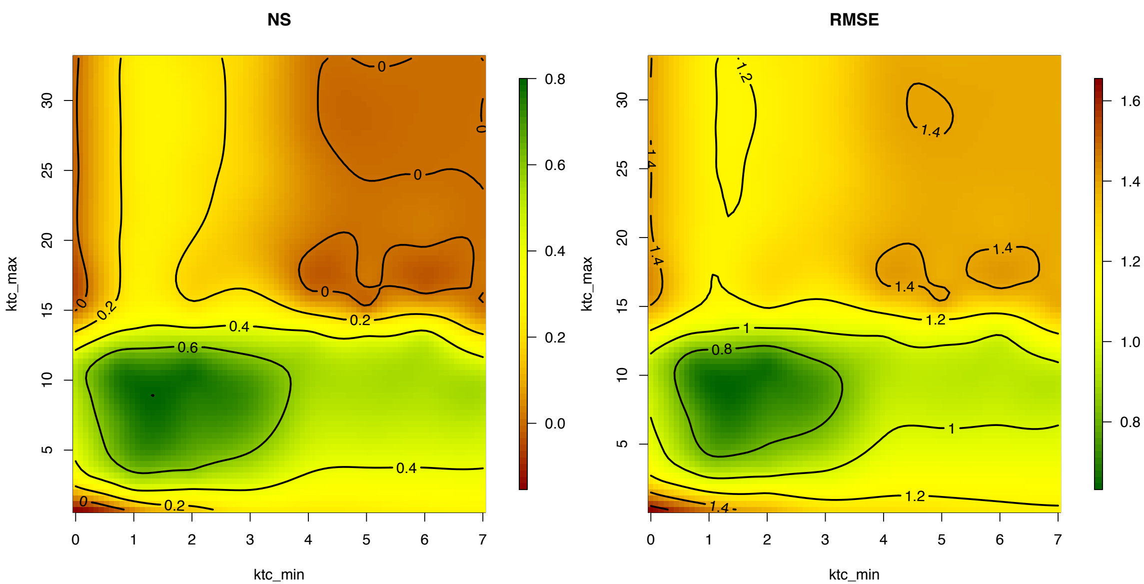

Figure 4

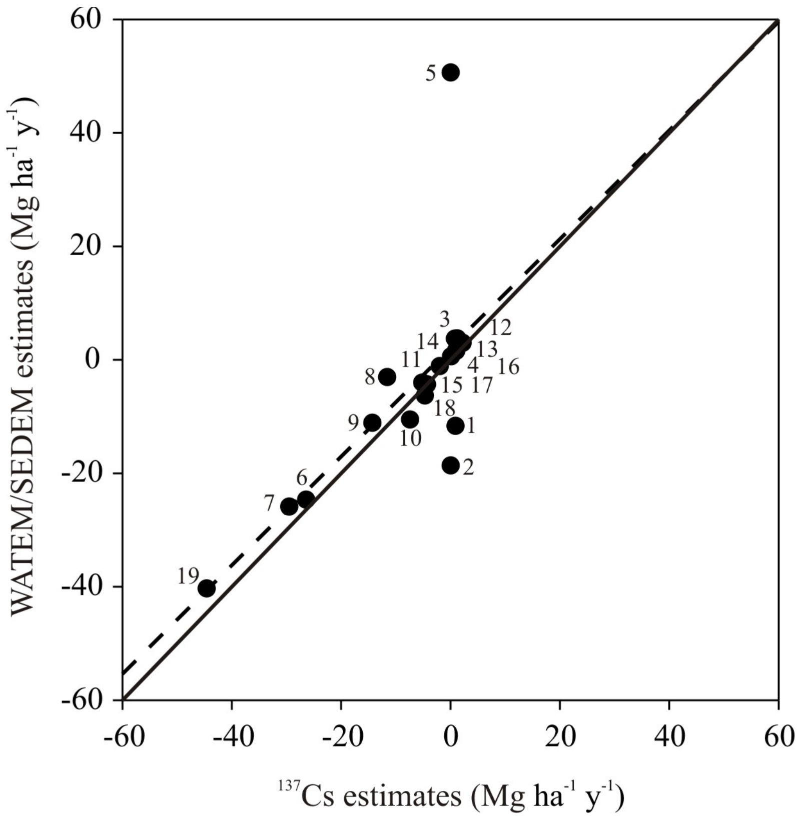

WATEM/SEDEM estimates (Mg ha-1 y-1)
137Cs estimates (Mg ha-1 y-1)
60
40
20
0
-20
-40
-60
-60
-40
-20
0
20
40
60
1
2
3
4
5
6
7
8
9
10
11
12
13
14
15
16
17
18
19

Figure 5

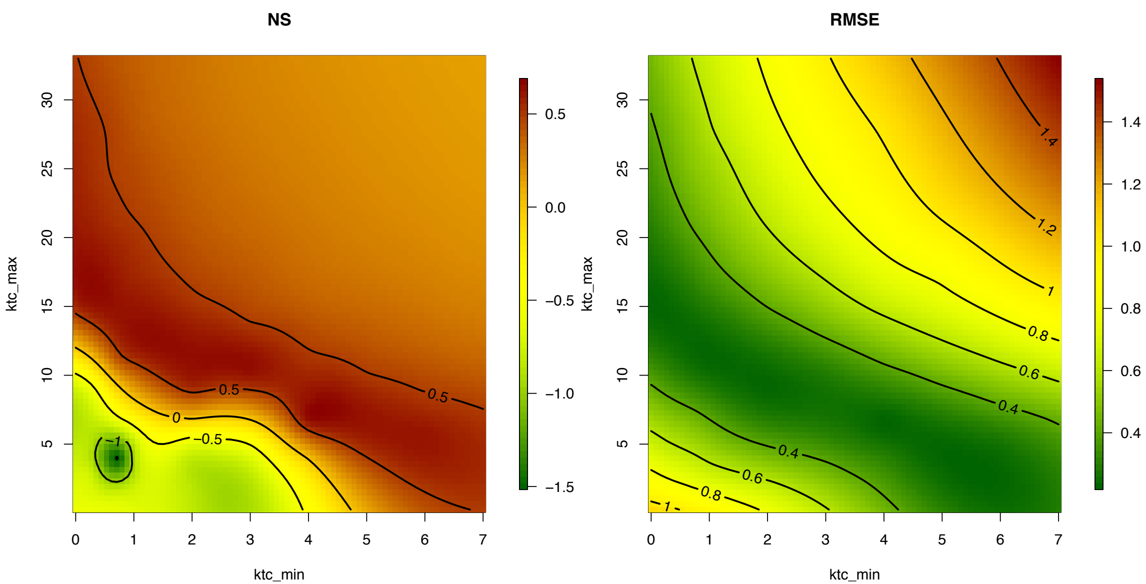

Figure 6

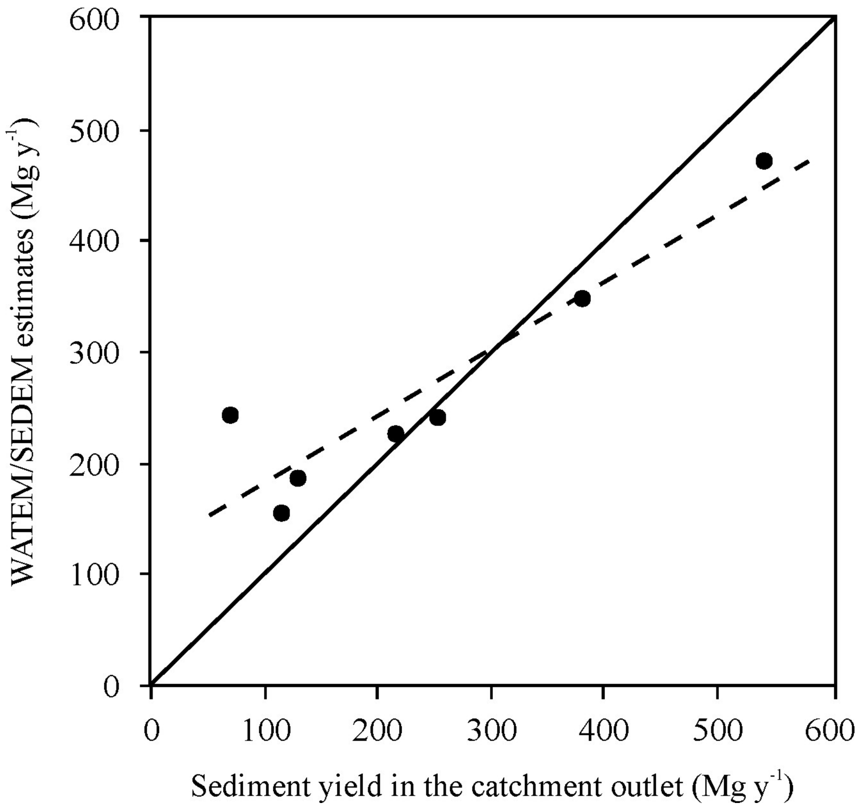
WATEM/SEDEM estimates (Mg y-1)
Sediment yield in the catchment outlet (Mg y-1)
0
100
200
300
400
500
600

Figure 7

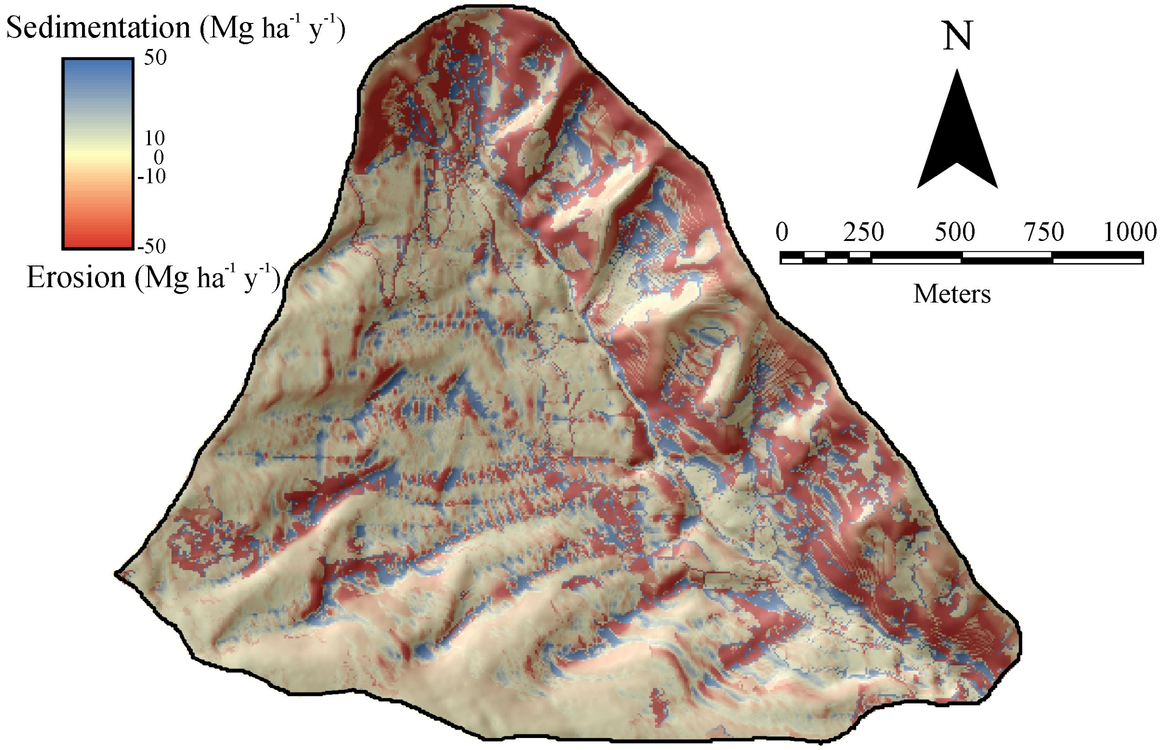

Sedimentation (Mg ha-1 y-1)
50
10
0
-10
-50
Erosion (Mg ha-1 y-1)
N
0
250
500
750
1000
Meters

Figure 8.


A)
Fields under agriculture
B)
River and bodies water
Forest
Road infrastructure
and build-up areas
Scrubland with high density

Figure 9

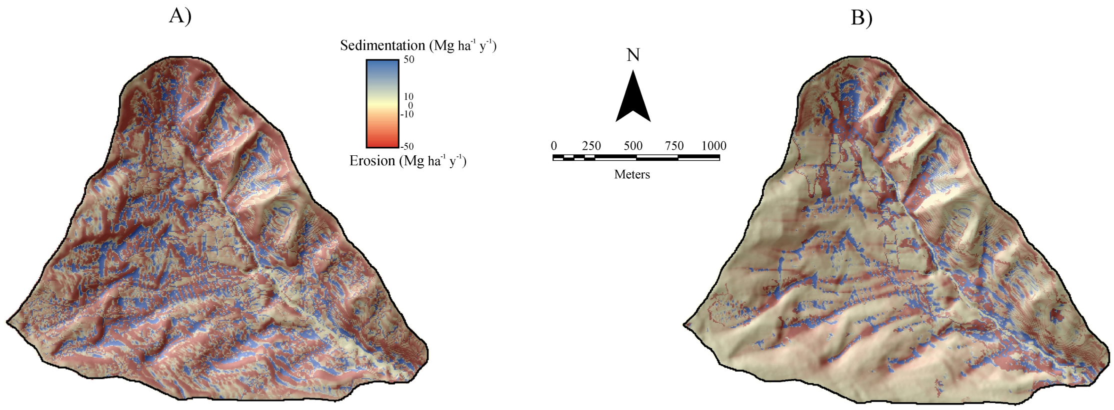
A)
B)
Sedimentation (Mg ha-1 y-1)
50
10
0
-10
-50
Erosion (Mg ha-1 y-1)
N
0 250 500 750 1000
Meters

Supplementary material

1. Generation of input maps for WATEM/SEDEM

1.1 Digital Elevation Model

The DEM plays a central role in WATEM/SEDEM, since it is used to calculate the slope gradient and the length−slope factor (LS_{2D}), and for routing the sediment downstream. We used a DEM with a spatial resolution of 1 m elaborated by the Spanish Ministry of Agriculture using photogrammetric restitution. The grid resolution of the DTM was then reduced to 5 × 5 m grid by averaging the values on the original grid. A pit-filling algorithm (Planchon and Darboux, 2001) was used to guarantee the hydrological connectivity of the grid cells until the catchment outlet.

1.2 Stream network

A map of the stream network was generated using the RUNOFF module in IDRISI, with the assumption that an upstream catchment area greater than a fixed value defined a channel. After testing different values, we concluded that a threshold area of 1 km^2 constituted a good approximation, since it showed good consistency with the stream network as seen in the orthophoto map of the catchment. The 1 km^2 threshold represents an upper limit beyond which sediment deposition is highly unlikely because of concentrated overland flow (Verstraeten et al., 2007).

1.3 Parcel map

The parcel map was a reclassification of the current land uses/land cover map (Figure 2B), which was derived from aerial orthophotos (SIGPAC, 2003). The aerial orthophotos were digitized and the LULC types were grouped into five major classes: cultivated land, forest, grassland, infrastructure and built-up areas, and water bodies. The original map was resampled to match the spatial resolution used in the study, using the RESAMPLE algorithm implemented in IDRISI.

1.4 Soil erodibility (K-factor)

The soil erodibility factor (K-factor of the RUSLE model) describes the susceptibility of soil to erosion by rainfall. Because of the lack of detailed soil maps it was necessary to analyze soil samples from the study area. A total of 77 bulk soil cores were collected on a grid pattern at the intersections of a 200 m × 200 m grid (Figure 1B), to assess the spatial distribution of physico-chemical soil properties relevant to soil erosion. To provide a database for the automated land evaluation system several main soil properties were analyzed in a previous study (Navas et al., 2005).

K-factor values were determined from soil texture data (Römkens et al., 1987) according to:

$$K_{text} = 0.0034 + 0.0405 \exp\left[-0.5\left(\frac{\log D_g + 1.659}{0.71}\right)^2\right], \qquad (1)$$

where K_{text} is a soil erodibility factor (Mg h MJ^{-1} mm^{-1}) and D_g is the geometric mean weight diameter of the primary soil particles (fraction < 2 mm). D_g was determined using a Coulter laser diffraction particle size analyzer (Coulter LS 230) for the 2–2000 μm fraction, following removal of organic matter (Buurman et al., 1997). K-factor values were then corrected to reflect the effect of stones in the soil surface on soil erodibility (Box, 1981):

$$K = K_{text} \exp^{(-0.0278 St)}, \qquad (2)$$

where *St* is the weight of stones in the topsoil, expressed as a percentage of the total weight of the topsoil. A K-factor map for the study area was obtained from the 77 selected sample points estimations by using a smoothing splines spatial interpolation method (Figure 2C).

1.5 Rainfall erosivity (R-factor)

The rainfall erosivity factor (R-factor, MJ mm ha^{-1} h^{-1} y^{-1}) is used to represent the impact of rain on soil erosion, and is based on the rainfall amount and intensity. The R-factor value was calculated for the area using a database of rainfall series from the SAIH system (automatic hydrological information network) of the Ebro basin water authority (Confederación Hidrográfica del Ebro). We used all available data to calculate R-factor values for the period October 1963 to September 2008. No high resolution (e.g. hourly) data were available, so we used an approximation based on daily rainfall data (Angulo-Martínez and Beguería, 2009). This way, an average R-factor of 1217 MJ mm ha^{-1} h^{-1} y^{-1} was used.

1.6 Crop management (C-factor)

A crop management factor (C-factor) was used to define the susceptibility of various LULC types to erosion by water. C-factor values were applied to each land use category according to the values proposed by the Spanish Institute for Nature

Conservation, ICONA (Almorox et al., 1994): 0 for water bodies and infrastructure built-up areas (i.e. no erosion); 0.003−0.030 for forest land cover; 0.030−0.250 for scrubland; 0.045−0.150 for grassland; and 0.250−0.800 for bare soil categories (Table 2). A C-factor map was constructed by applying those values to the LULC map (Figure 2D).

1.7 Model efficiency statistics

The Nash-Sutcliffe statistic was computed as:

$$NS = 1 - \frac{\sum_{i=1}^{n} (O_i - P_i)^2}{\sum_{i=1}^{n} (O_i - O_{mean})^2}, \quad (3)$$

where n is the number of observations, O_i is the observed value, O_{mean} is the mean observed value, and P_i is the predicted value. The value of NS can range from $-\infty$ to 1, and represents the proportion of the initial variance accounted for by the model. The closer the value of NS is to 1, the more efficient is the model in reproducing the observed values.

The relative root mean square error was computed as:

$$RRMSE = 1 - \frac{\sqrt{\frac{1}{n}\sum_{i=1}^{n} (O_i - P_i)^2}}{\frac{1}{n}\sum_{i=1}^{n} O_i}. \quad (4)$$